Behavior Modeling and Digital Predistortion of Mismatched Wireless Transmitters Using Convolutional Neural Networks

Praveen Jaraut, *Senior Member, IEEE*, Sagar K. Dhar, *Member, IEEE*, Mohamed Helaoui, *Senior Member, IEEE*, Noureddine Boulejfen, *Senior Member, IEEE*, Meenakshi Rawat, *Member, IEEE*, Wenhua Chen, *Senior Member, IEEE*, Karun Rawat, *Senior Member, IEEE*, Noureddine Outaleb, and Fadhel M. Ghannouchi, *Fellow, IEEE*

***Abstract*—In modern wireless compact transmitters, Power Amplifier (PA) behavior is considerably affected by the impedance mismatch between the PA's output and the antenna's input. This PA's output mismatch results in a reflection at the PA–antenna interface. In this brief, reflection-aware PA modeling and digital predistortion (DPD) techniques are proposed to mitigate the negative impact of this mismatch on the forward and reverse models of the PA. An Augmented Convolutional neural network model (ΓACNN) is proposed to linearize a Doherty PA under different values of the output mismatch using a single set of coefficients. The developed DPD shows robust performance metrics like normalized mean square error (NMSE), and adjacent channel power ratio (ACPR) under diverse complex output mismatch levels.**

***Index Terms*—Convolutional neural network (CNN), digital predistortion (DPD), linearization, output mismatch, power amplifier (PA), wireless transmitters.**

I. Introduction

IN WIRELESS transmitters, Power Amplifiers (PAs) contributes most of the nonlinear distortions. These nonlinear distortions adversely affect the system's aggregate performance. Digital Predistortion (DPD) has been a popular technique for improving PA performance for many years. The DPD improves the PA linearity in the high-efficiency region, and it is performed in the digital domain [1]. Most of the research work to develop the DPD technique and improve their performance considers a perfect-matched condition. However, the output of the PA might not be perfectly matched. This output mismatch results in unpredicted reflections, reducing output power and efficiency and producing nonlinear distortions [2], [3], [4]. Thus, degrading the overall performance of the system. Although isolators can mitigate the reflection of the signal but they are primarily narrowband, costly, bulky, often cannot be integrated into systems. They make it more challenging to design transmitters with multiband and wideband capabilities. Therefore, isolator-free PAs using DPD techniques are necessary to manage the output mismatch.

The PA modeling and DPD performance degrade under a reflection coefficient as low as $\Gamma = 0.2$ [5]. In [6], [7], [8], [9], the poly-harmonic distortion (PHD) model is used to determine the PA behavior under different load mismatches, but this model is most appropriate when dynamic PA behavior is ignored. In [10], a dynamic dual-input model is proposed, which takes into account a first-order estimate of the reflected signal at the output port. The performance of this model is restricted to a low reflection coefficient. In [11], a more improved dual-input model is proposed to manage output mismatch effects. This model requires a higher number of coefficients, and it increases numerical instability due to the inversion of a large observation matrix. This dual-input model is optimized in [12]. This optimized model considers a second-order estimate of the reflected signal at the output port for a tradeoff between accuracy and complexity. The higher value of reflection degrades the performance of these dual-input models. In [13], a dual-input crossover memory polynomial (COMP) DPD is proposed to linearize PA with different load mismatches. However, a unique set of coefficients is derived for each training load mismatch condition. After that, these sets of model coefficients obtained for different load mismatch conditions are interpolated to cover a continuous range of load mismatch conditions. The disadvantage of this model is that it requires multiple sets of model coefficients for multiple training loads' mismatches. In [14], an augmented convolutional neural network (ACNN) is proposed to linearize the multi-band PA transmitter. The inputs of the model presented in [14] are only the baseband $I(n)$ and $Q(n)$ and their delayed versions for all the carriers. In [14], the model does not

Manuscript received 17 July 2022; revised 20 August 2022; accepted 6 September 2022. Date of publication 19 September 2022; date of current version 22 December 2022. This work was supported in part by the Alberta Innovates Technology Futures, Canada, and in part by the National Science and Engineering Research Council, Canada. This brief was recommended by Associate Editor L. A. Camunas-Mesa. *(Corresponding author: Praveen Jaraut.)*

Praveen Jaraut, Mohamed Helaoui, and Fadhel M. Ghannouchi are with the Department of Electrical and Software Engineering, University of Calgary, Calgary, AB T2N 1N4, Canada (e-mail: praveen.jaraut@ieee.org; mhelaoui@ucalgary.ca; fghannou@ucalgary.ca).

Sagar K. Dhar is with the RF Power Group, Renesas Electronics, San Diego, CA 92121 USA.

Noureddine Boulejfen is with the Military Research Center, Ministry of Defense, Tunis 2045, Tunisia (e-mail: nboulejf@ieee.org).

Meenakshi Rawat and Karun Rawat are with the Electronics and Communication Department, Indian Institute of Technology Roorkee, Roorkee 247667, India.

Wenhua Chen is with the Department of Electronic Engineering, Tsinghua University, Beijing 100084, China (e-mail: chenwh@tsinghua.edu.cn).

Noureddine Outaleb is with the Wireless Systems Group, Analog Device Inc., Ottawa, ON K2B 6B7, Canada (e-mail: noureddine.outaleb@analog.com).

Color versions of one or more figures in this article are available at https://doi.org/10.1109/TCSII.2022.3207525.

Digital Object Identifier 10.1109/TCSII.2022.3207525

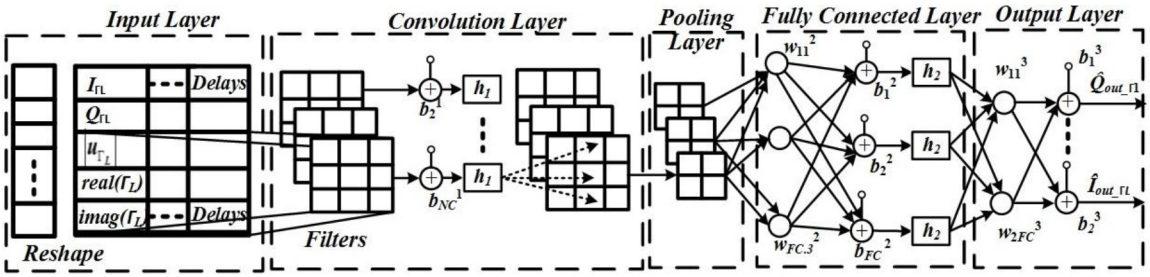

Fig. 1. The Architecture of ΓACNN.

consider the environment (e.g., temperature [15]) and the setting (e.g., impedance mismatch, biasing, etc.) conditions of the power amplifier (PA) that vary in field applications and impacts significantly the performance of the PA and hence the DPD compensator. In contrast to the proposed work, the mismatch at the output of the amplifier, Γ, is added as an input parameter to the proposed ΓACNN.

This brief proposes a novel Augmented Convolutional Neural Network (ΓACNN) with application to a DPD for PAs with output mismatch, which has better linearization performance than existing DPD models. The proposed DPD requires a single set of model coefficients for different load mismatches than multiple sets of model coefficients required by COMP DPD [13]. The input of ΓACNN has a reflection coefficient (Γ). A convolutional layer, a pooling layer, a hidden fully connected layer, and an output layer are all part of the proposed ΓACNN DPD. The robust adjacent channel power ratio (ACPR) and normalized mean square error (NMSE) are the linearization performances of the proposed ΓACNN DPD.

This brief is organized as follows: Section II discusses the state-of-the-art models followed by the proposed model. Section III presents the measurement setup used. Section IV shows the behavioral modeling and linearization performances of the proposed reflection-aware model for different output mismatches. After that, the conclusion is presented in Section V.

II. Proposed Models

A. State-of-the-Art Models

The Memory Polynomial (MP) model is mathematically expressed as

$$y(n) = \sum_{\tau=0}^{M} \sum_{k=0}^{K} a_{mk} u(n-\tau)|u(n-\tau)|^k \tag{1}$$

where M, K, $u(n)$ and $y(n)$ denote the memory depth, nonlinearity order, baseband input signal, and baseband output signal, respectively.

The reflection coefficient (Γ) can be mathematically expressed as

$$\Gamma = \frac{a_2}{b_2} = \frac{Z_L - Z_{out}^*}{Z_L + Z_{out}} \tag{2}$$

where a_2, b_2, Z_L and Z_{out} are the reflected wave, incident wave, load impedance, and PA output impedance, respectively.

The COMP model [13] is mathematically expressed as

$$y(n) = \sum_{\tau=0}^{M_1} \sum_{k=0}^{K_1} \alpha_{mk}(\Gamma) u(n-\tau)|u(n-\tau)|^k |u_2(n-\tau)|^k + \sum_{\tau=0}^{M_2} \sum_{k=0}^{K_2} \beta_{mk}(\Gamma) u_2(n-\tau)|u(n-\tau)|^k |u_2(n-\tau)|^k \tag{3}$$

where M_1, M_2, K_1, K_2, $u_2(n)$, $\alpha_{mk}(\Gamma)$ and $\beta_{mk}(\Gamma)$ denotes the memory depths, nonlinearity orders, baseband reflected output signal of the PA, and model coefficients, respectively.

The disadvantage of this model is that it requires the extraction of multiple sets of model coefficients ($\alpha_{mk}(\Gamma)$ and $\beta_{mk}(\Gamma)$) for each value of training load points. These sets of model coefficients are used to interpolate for testing load points.

B. Proposed Models

Generally, the ACNN model's input layer comprises past and present values of baseband input signals and their amplitudes [14].

The input matrix of the ACNN model is mathematically expressed as

$$U = [I(n), Q(n), |u(n)|, \ldots, Delays] \tag{4}$$

where I, Q and $|u|$ are the real, imaginary, and amplitude of baseband input signal.

The input matrix of the ACNN used for different reflection coefficients Γ_1, Γ_2 .... Γ_L is mathematically expressed as

$$\tilde{U} = [I_{\Gamma_1}, \ldots I_{\Gamma_L}, Q_{\Gamma_1}, \ldots Q_{\Gamma_L}, |u_{\Gamma_1}|, \ldots |u_{\Gamma_L}|, \ldots, Delays] \tag{5}$$

To include the effects of the output mismatch, the input matrix of the ΓACNN model used for training is

$$\check{U} = \big[I_{\Gamma_1}, \ldots I_{\Gamma_L}, Q_{\Gamma_1}, \ldots Q_{\Gamma_L}, |u_{\Gamma_1}|, \ldots |u_{\Gamma_L}|, real(\Gamma_1), \ldots real(\Gamma_L), imag(\Gamma_1), \ldots imag(\Gamma_L),, \ldots, Delays\big] \tag{6}$$

The input layer of the ΓACNN architecture consists of past and present values of I_1, ... I_L, Q_1, ... Q_L, $|u_1|$,... $|u_L|$, real(Γ_1), ... real(Γ_L), imag(Γ_1), ... imag(Γ_L) as shown in the Fig. 1. Instead of choosing reflection-dependent model coefficients in [13], the reflection coefficient is included as the model's input. This will result in a single set of coefficients for different output mismatches.

The architecture of the ΓACNN model is represented in Fig. 1. In the Input layer, these input terms are reorganized into a two-dimensional matrix to form an image. The input is convolved with the weights of the filter in the convolutional layer, and then the bias is applied. The hyperbolic tangent activation function h_1 uses this convolution sum as its input [14]. Each filter slides with a stride over the input layer, and previous operations are repeated. The pooling layer is then utilized to reduce the convolutional output matrix. The average pooling's output is linked to all of the fully connected layer's neurons. The activation function h_2 of the fully connected layer is also the hyperbolic tangent function [14]. The reduction of the size

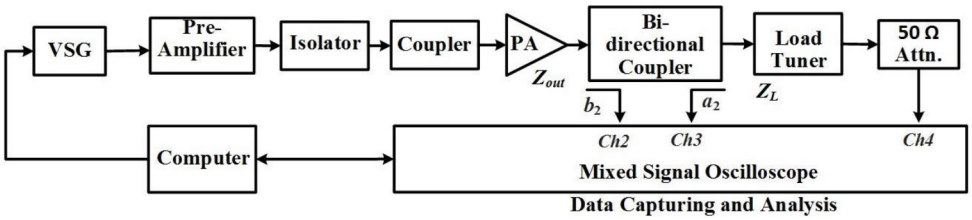

Fig. 2. Block Diagram of the experimental setup.

of the convolutional output matrix by the pooling layer results in the decrease of the number of weights and computations in the fully connected layer. The activation function for the ACNN's final output layer is a linear function. The ADAM algorithm is used to update back propagation's weights and biases quickly [14], [15], [16].

III. Experimental Setup

Fig. 2 displays the block diagram of the experimental setup. The N5182A MXG vector signal generator transmits the modulated input signal. The 20 MHz, four carrier QAM modulated signal has a peak to average power ratio (PAPR) of 11.25 dB and a sampling rate of 92.16 MHz. It is transmitted at 2.14 GHz carrier frequency to drive the DUT (20–W Doherty PA) over a gain compression of roughly 2.6 dB for a 50 Ω termination. However, due to different load terminations, the gain compression changes from 2 dB to 5 dB. Many load points are attainable by calibrating the load tuner MPT 1818 using the N5230A PNA network analyzer. It emulates the output mismatch conditions. The data capturing and analysis block includes the MS09404A mixed-signal oscilloscope to capture the output y (channel 4), reflected b_2 (channel 2), and incident a_2 (channel 3) signals using the. PathWave 89600 VSA software.

IV. Experimental Results

A. Behavioral Modeling Results

The behavioral PA model is extracted, and its performance is calculated by applying the following steps: 1) capture the waveforms of the input and output of the PA under various load reflection terminations (training loads); 2) record the actual reflection coefficient (Γ) of each training load point along with its input and output waveforms, 3) derive a single set of model coefficients; and 4) for a given test load point, calculate the NMSE between the measured and modeled outputs [17]. As single set of model's coefficients are calculated for the proposed ΓACNN model for different values of training load mismatches. Thus it reduces the total number of coefficients.

Both the phase and magnitude of the reflection coefficient (Γ) are essential for the behavioral modeling of PA. The phase has been swept from 0° to 360°, while the magnitude of Γ has been swept from 0.05 to 0.35. The performances of the MP w/o Γ, COMP, and ΓACNN models have been assessed for two cases. In case I, training load points and testing load points are the same. In case II, the number of training load points is one-third of the testing load points.

Fig. 3 shows the obtained NMSE values for the case I in PA behavioral modeling. 2000 samples for each Γ have been used during the training stage to extract the model coefficients, while 131072 samples have been used for model testing for each Γ value. The MP model w/o Γ using (1) is tested for M=3 and K=6. The COMP model is tested for M_1=3, M_2=3, K_1=6, and K_2=4 with a single set of coefficients and multiple sets of model's coefficients using (3). The proposed ΓACNN model is tested for L_1=7, L_2=2, C_1=4, C_2=1, N_C=3, F_C=3, P_o=2, Z_P=0, S_t=1, M=3 with a single set of coefficients, where $L_1 \times L_2$ is the size of the input layer, $C_1 \times C_2$ is the convolutional filter's size, N_C is the number of convolutional filters, F_C is the number of neurons of fully connected layer, P_o is the pooling factor, Z_P is the number of zero padding, and S_t is the number of strides. The performance of the COMP model with a single set of model's coefficients degrades as compared to the COMP with interpolated multiple sets of model's coefficients. The proposed ΓACNN model with a single set of coefficients has better NMSE than other models for different values of Γ. Also, the proposed ΓACNN has robust NMSE performance over Γ.

TABLE I
Behavioral Modeling Results for Different Models

	MP w/o Γ (Case I)	COMP w/ single set (Case I)	COMP w/ multiple sets (Case I)	ΓACNN (Case I)	COMP w/ multiple sets (Case II)	ΓACNN (Case II)
Average NMSE (dB)	-20.25	-22.23	-27.93	-34.15	-26.74	-31.99
No. of Coeff	28	48	1440	44	480	44

Fig. 4 shows the NMSE between the measured and the modeled output for case II. Also, 2000 samples are used for each training load, and 131072 samples are used for each testing load. The proposed ΓACNN model with a single set of coefficients has better NMSE than the COMP model with multiple sets of coefficients for different values of Γ. Again, the proposed ΓACNN has robust NMSE performance over Γ.

Table I shows the average NMSE of the different models over the whole considered range of Γ. In case I, the average NMSE for the ΓACNN model is lower than the MP, COMP model with a single set of coefficients and multiple sets of model's coefficients by 14 dB, 12 dB, and 6 dB respectively. The total number of coefficients of the COMP model with multiple sets of coefficients increases significantly as many times the number of testing load points. The proposed ΓACNN model requires fewer coefficients than the COMP model with a single set of coefficients and multiple sets of model's coefficients. In case II, the ΓACNN model outperforms the COMP model by a 5 dB lower average NMSE.

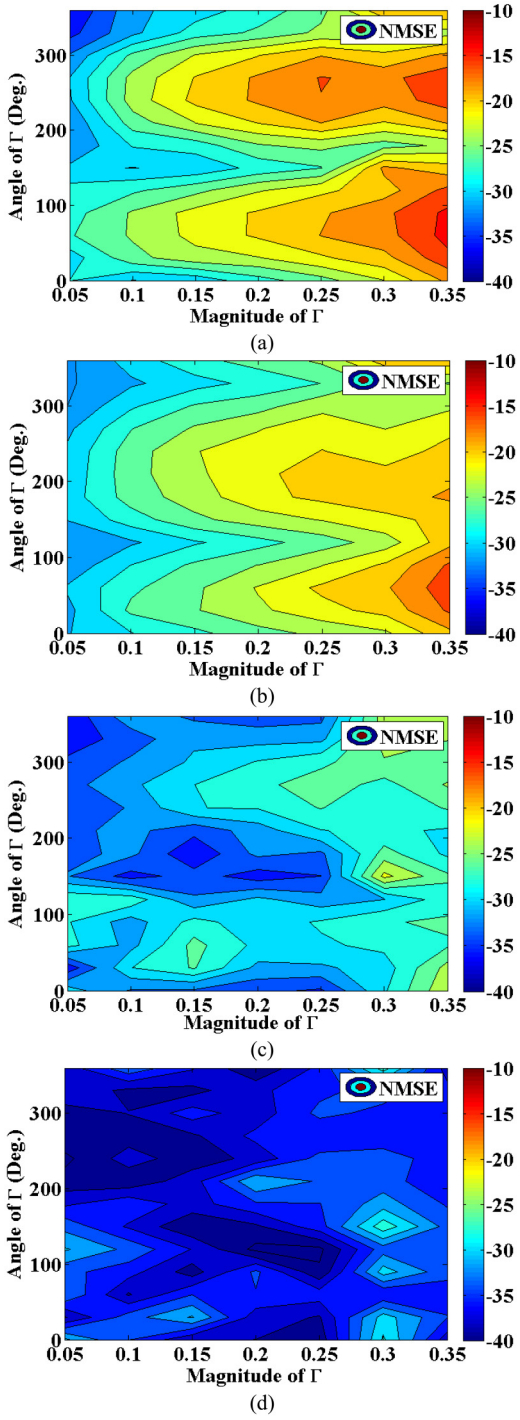

Fig. 3. NMSE of the (a) MP model without Γ, (b) COMP model with single set of coefficients, (c) COMP model with multiple sets of coefficients, and (d) ΓACNN model in case I.

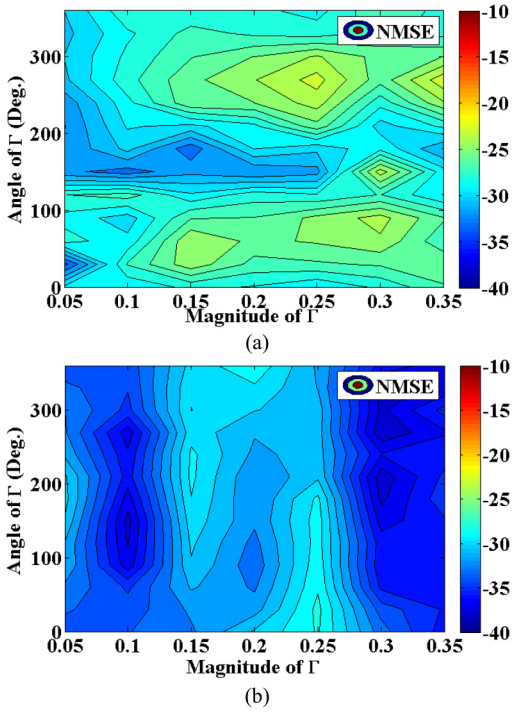

Fig. 4. NMSE of the (a) COMP model with multiple sets of coefficients and (b) ΓACNN model in case II.

TABLE II
DPD RESULTS FOR DIFFERENT MODELS

	MP w/o Γ (Case I)	COMP w/ single set (Case I)	COMP w/ multiple sets (Case I)	ΓACNN (Case I)	COMP w/ multiple sets (CaseII)	ΓACNN (Case II)
Average NMSE (dB)	-19.87	-21.37	-27.78	-32.91	-25.52	-31.32
No. of Coeff	28	48	1440	44	480	44

B. DPD Results

The indirect learning architecture has been applied using the least-squares method to perform the DPD coefficients extraction. In indirect learning DPD, a set of reverse model coefficients is extracted for different training load points. Then the testing load is changed, and the linearization performances are calculated for MP, COMP, and ΓACNN DPDs.

Table II shows the average NMSE of different DPDs over the whole considered range of Γ such that $|\Gamma| \in [0.05, 0.35]$ and $\angle\Gamma \in [0, 360^0]$. The MP DPD w/o Γ is tested for M=3 and K=6. The COMP DPD is tested for M_1=3, M_2=3, K_1=6, and K_2=4 with a single set of coefficients and multiple sets of DPD's coefficients. The proposed ΓACNN DPD is tested for L_1=7, L_2=2, C_1=4, C_2=1, N_C=3, F_C=3, P_o=2, Z_P=0, S_t=1, M=3 with a single set of DPD coefficients. In case I, the average NMSE for the ΓACNN DPD is lower than those of the MP and COMP DPDs with a single set of coefficients and multiple sets of coefficients by 13 dB, 11 dB and 5 dB, respectively. The proposed ΓACNN DPD requires fewer coefficients than the COMP DPD with a single set of coefficients and multiple sets of coefficients. In case II, the average NMSE for ΓACNN DPD is lower than that of the COMP DPD by 6 dB.

Fig. 5 shows the normalized power spectral density (PSD) of various DPDs at three different load values (Γ=0.35∠180°, 0.35∠270° and 0.15∠60) in case II. Table III shows the ACPR values at three different load values (Γ=0.35∠180°, 0.35∠270° and 0.15∠60) for case II. From Fig. 5 and Table III, the proposed ΓACNN DPD has better ACPR by 8 dBc, 13 dBc and 12 dBc than the MP w/o Γ DPD at Γ=0.35∠180°, 0.35∠270° and 0.15∠60 respectively. Similarly, the proposed ΓACNN DPD has better ACPR by 3 dBc, 7 dBc and 6 dBc than COMP with multiple sets of

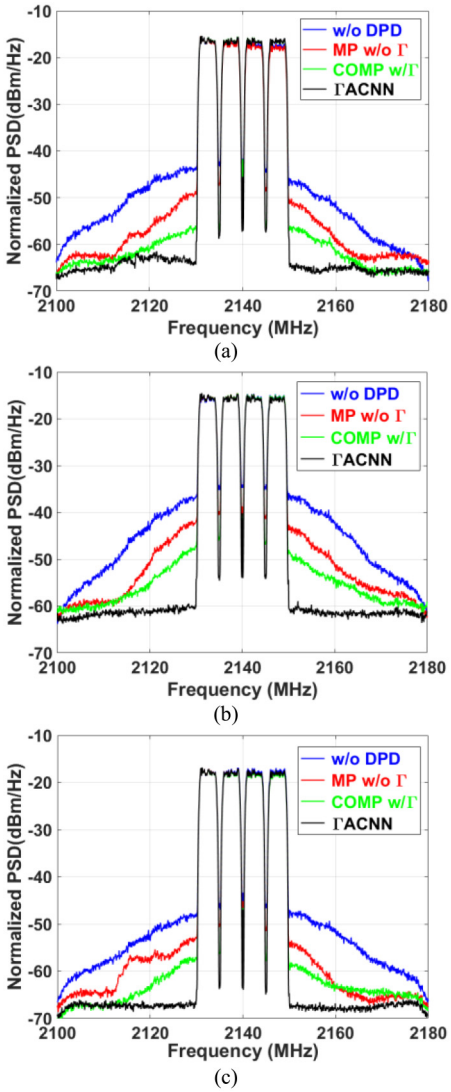

Fig. 5. DPD at (a) 0.35∠180°, (b) 0.35∠270°, and (c) 0.15∠60° in Case II.

TABLE III
ACPR RESULTS FOR DIFFERENT DPDS

Testing Load Γ_L	ACPR			
	w/o DPD	MP w/o Γ (Case II)	COMP w/ multiple sets (Case II)	ΓACNN (Case II
0.35∠180°	-31.25	-40.85	-45.03	-48.21
0.35∠270°	-28.35	-33.59	-39.15	-46.04
0.15∠60°	-33.58	-38.68	-44.29	-50.53

DPD coefficients at Γ=0.35∠180°, 0.35∠270° and 0.15∠60 respectively.

V. CONCLUSION

The mismatch between the output of the amplifier and the antenna's input is a practical design impairment of wireless transmitters. It leads to deterioration in the modeling and linearization performances of the transmitter when no isolator is used to shield the amplifier from any antenna mismatch. This amplifier-antenna mismatch is modeled in PA behavioral modeling, and DPD is performed to linearize PA. The performance of the proposed ΓACNN DPD using a single set of coefficients is tested under a broad range of load mismatches. The proposed model enhances linearization performance in terms of ACPR and NMSE by 3–7 dBc and 6 dB, respectively, under such varied situations. Despite the proposed approach is tested for single-input single-output (SISO) transmitters, it can also be extended to mitigate the antenna elements' cross-talk and mismatch effects in multi-input multi-output (MIMO) phased array-based transmitters.

REFERENCES

[1] F. M. Ghannouchi, O. Hammi, and M. Helaoui, *Behavioral Modeling and Predistortion of Wideband Wireless Transmitters*. Hoboken, NJ, USA: Wiley, 2015.

[2] C. Sanchez-Perez *et al.*, "Dynamic load modulation with a reconfigurable matching network for efficiency improvement under antenna mismatch," *IEEE Trans. Circuits Syst. II, Exp. Briefs*, vol. 58, no. 12, pp. 892–896, Dec. 2011.

[3] A. van Bezooijen, R. Mahmoudi, and A. H. M. van Roermund, "Adaptive methods to preserve power amplifier linearity under antenna mismatch conditions," *IEEE Trans. Circuits Syst. I, Reg. Papers*, vol. 52, no. 10, pp. 2101–2108, Oct. 2005.

[4] A. Suárez, F. Ramírez, and S. Sancho, "Stability analysis of power amplifiers under output mismatch effects," *IEEE Trans. Microw. Theory Techn.*, vol. 62, no. 10, pp. 2273–2289, Oct. 2014.

[5] E. Zenteno, M. Isaksson, and P. Händel, "Output impedance mismatch effects on the linearity performance of digitally predistorted power amplifiers," *IEEE Trans. Microw. Theory Techn.*, vol. 63, no. 2, pp. 754–765, Feb. 2015.

[6] M. Romier, A. Barka, H. Aubert, J. P. Martinaud, and M. Soiron, "Load-pull effect on radiation characteristics of active antennas," *IEEE Antennas Wireless Propag. Lett.*, vol. 7, pp. 550–552, 2008.

[7] G. Z. El Nashef *et al.*, "EM/circuit mixed simulation technique for an active antenna," *IEEE Antennas Wireless Propag. Lett.*, vol. 10, pp. 354–357, 2011.

[8] J. Verspecht and D. E. Root, "Polyharmonic distortion modeling," *IEEE Microw. Mag.*, vol. 7, no. 3, pp. 44–57, Jun. 2006.

[9] D. E. Root, J. Verspecht, D. Sharrit, J. Wood, and A. Cognata, "Broadband poly-harmonic distortion (PHD) behavioral models from fast automated simulations and large-signal vectorial network measurements," *IEEE Trans. Microw. Theory Techn.*, vol. 53, no. 11, pp. 3656–3664, Nov. 2005.

[10] C. Fager *et al.*, "Prediction of smart antenna transmitter characteristics using a new behavioral modeling approach," in *IEEE MTT-S Int. Microw. Symp. Dig.*, Jun. 2014, pp. 1–4.

[11] H. Zargar, A. Banai, and J. C. Pedro, "A new double input-double output complex envelope amplifier behavioral model taking into account source and load mismatch effects," *IEEE Trans. Microw. Theory Techn.*, vol. 63, no. 2, pp. 766–774, Feb. 2015.

[12] J. Cai, R. Gonçalves, and J. C. Pedro, "A new complex envelope behavioral model for load mismatched power amplifiers," *Int. J. RF Microw. Comput.-Aided Eng.*, vol. 27, no. 6, 2017, Art. no. e21097.

[13] S. K. Dhar *et al.*, "A reflection-aware unified modeling and linearization approach for power amplifier under mismatch and mutual coupling," *IEEE Trans. Microw. Theory Techn.*, vol. 66, no. 9, pp. 4147–4157, Sep. 2018.

[14] P. Jaraut *et al.*, "Augmented convolutional neural network for behavioral modeling and digital predistortion of concurrent multi-band power amplifiers," *IEEE Trans. Microw. Theory Techn.*, vol. 69, no. 9, pp. 4142–4156, Sep. 2021.

[15] A. Motaqi, M. Helaoui, N. Boulejfen, W. Chen, and F. M. Ghannouchi, "Artificial intelligence-based power-temperature inclusive digital predistortion," *IEEE Trans. Ind. Electron.*, vol. 69, no. 12, pp. 13872–13880, Dec. 2022.

[16] Z. Liu *et al.*, "Low computational complexity digital predistortion based on convolutional neural network for wideband power amplifiers," *IEEE Trans. Circuits Syst. II, Exp. Briefs*, vol. 69, no. 3, pp. 1702–1706, Mar. 2022, doi: 10.1109/TCSII.2021.3109973.

[17] P. L. Gilabert, D. López-Bueno, and G. Montoro, "Spectral weighting orthogonal matching pursuit algorithm for enhanced out-of-band digital predistortion linearization," *IEEE Trans. Circuits Syst. II, Exp. Briefs*, vol. 66, no. 7, pp. 1277–1281, Jul. 2019.